# Improved Electrochemical Performance of Modified Mesocarbon Microbeads for Lithium-Ion Batteries Studied using Solid-State Nuclear Magnetic Resonance Spectroscopy

Katharina Bösebeck,*[a] C. Vinod Chandran,[a] Björn K. Licht,[b] Michael Binnewies,[b] and Paul Heitjans*[a]

Lithium-intercalating materials such as graphite are of great interest, especially for application in lithium-ion batteries. In this work we present an investigation of the electrochemical performance of mesocarbon microbeads (MCMB) modified with copper to reveal the basic electrochemical mechanisms. Copper-modified graphite is known to have better long-term cycling behavior as well as higher capacity compared to the pristine material. Several reasons for these effects were postulated but not proven. Solid-state nuclear magnetic resonance (NMR) spectroscopy provides structural and dynamic information on lithium in ionic conductors. To elucidate the changes in structure and dynamics for the pristine and the modified material, we have employed multi-nuclear solid-state NMR spectroscopy as well as $^{7}$Li spin-lattice relaxation measurements and were able to clarify some reasons for the improved characteristics of copper-modified graphite compared to the pristine material, which include increased solid–electrolyte interface (SEI) formation, a facilitated diffusion of lithium ions through the SEI, and reduced moisture.

## Introduction

To address the growing demand for high-capacity electrical energy storage, advanced battery materials are of essential need. A key to improving battery quality characteristics such as capacity or cycling stability is the better understanding of basic electrochemical processes in active materials. Besides the development of new materials, an active field of research is the modification of already-established electrode materials to improve their performance. In many cases, the influences of these modifications are well documented, whereas the mechanisms behind are often incompletely understood.

Successful attempts to improve the performance of graphite anode materials include modifications involving metals, metal oxides, secondary carbon shells, and silicon dioxide coatings.[1–4] The hypothesized reasons for the improvements due to these modifications include the reduction of mechanical stress, a change in the solid–electrolyte interface (SEI), and a reduction of co-intercalation of solvated lithium ions during cycling. It is also possible that nanostructured metals have a catalytic effect on the lithium intercalation. Licht et al.[5] demonstrated the suppression of the co-intercalation of solvated lithium ions using flake graphite modified with copper. The graphite used in this work is composed of mesocarbon microbeads (MCMB). MCMB are spherical particles of typically tens of micrometers in diameter and a promising material for battery applications.[6] Winter et al.[7] found that the thickness of the graphite particles has a great influence on the co-intercalation of solvated lithium ions. Therefore, the sole suppression of co-intercalation would have a relatively small impact on the cycle life and discharge capacity of the rather thick MCMB particles. Cycling experiments show a significantly higher discharge capacity and better long-term stability for MCMB modified with copper (MCMB_Cu) compared with pristine MCMB.

Solid-state nuclear magnetic resonance (NMR) spectroscopy is well known for providing structural and dynamic information on lithium in ionic conductors. The applied probe nuclei for these studies include $^{6}$Li, $^{7}$Li, and $^{8}$Li (see Ref. [8] for a recent review). There are several solid-state NMR studies on lithium intercalation in carbon matrices, for example graphite intercalation compounds (GICs).[9] The GICs, for different Li–C crystallographic environments, exhibit a range of Li chemical shielding and quadrupole interaction strengths

[a] K. Bösebeck, Dr. C. V. Chandran, Prof. Dr. P. Heitjans
Institut für Physikalische Chemie und Elektrochemie
Leibniz Universität Hannover
Callinstr. 3, 30167 Hannover (Germany)
E-mail: boesebeck@pci.uni-hannover.de
heitjans@pci.uni-hannover.de

[b] Dr. B. K. Licht, Prof. Dr. M. Binnewies
Institut für Anorganische Chemie
Leibniz Universität Hannover
Callinstr. 9, 30167 Hannover (Germany)



Part of a Special Issue on "Li-Ion Batteries". To view the complete issue, visit: http://dx.doi.org/10.1002/ente.v4.12

during Li insertion/removal steps.[10] This helps to characterize the structural properties whereas nuclear spin relaxation gives clues on the dynamics in the system. Depending on the extent of Li intercalation in GICs ($LiC_{6n}$ with $n=1, 2, 3.$) the $^{6/7}$Li chemical shifts vary between 0 and 45 ppm. The Li-rich GIC stages shift to higher chemical shift values. A smaller quadrupole coupling is typically associated with the Li-poor stage.[10,11] Conard et al. first described Li motion in $LiC_6$ using NMR.[12] They observed line narrowing of the $^7$Li central transition NMR signal at high temperatures. Later, the Li motion in $LiC_6$ was studied using β-radiation-detected $^8$Li spin-lattice relaxation (SLR) experiments and a twodimensional (2D) diffusion mechanism was proposed.[13] Faster Li-ion diffusion was always observed for $LiC_6$ than for $LiC_{12}$ with activation energies ($E_A$) of 0.6 and 1.0 eV, respectively.[14] An even smaller $E_A$ (0.4 eV) was deduced for Li diffusion in carbon nanotubes.[15] This evidences the influence of the dimensionality of the motion pathways and morphology on the ionic diffusion. In another study of $LiC_6$ using $^7$Li SLR and spin alignment echo (SAE) NMR experiments, the $E_A$ of the 2D diffusion process was confirmed to be 0.55 eV with a Li diffusion coefficient of $10^{-15}$ $m^2 s^{-1}$ at ambient conditions.[16]

A recent theoretical approach calculated the $E_A$ for Li hopping in $LiC_{6n}$, based on Frenkel defects (0.42–0.52 eV) and Li vacancies (0.42–0.56 eV).[17] Lithium intercalation in MCMB was investigated with $^7$Li NMR by Tatsumi et al.[18] and two main signals (at 27 and 45 ppm) were observed for the heat-treated samples (>2000 °C). Below a heat-treatment temperature of 700 °C, the $^7$Li signals shifted close to the 0–10 ppm range, even after full Li intercalation.[19] Li insertion in MCMB (heat treated below 700 °C) with a surface modified with citric acid moieties showed $^7$Li NMR signals in the range between −2 and 20 ppm after the first discharge (420 mAh $g^{-1}$) to 0.0 V at *C*/20 rate.[20] The main two signals centered at −2 and 3.5 ppm were attributed to Li in passivating layers (and traces of electrolyte) and in-between graphene layers, respectively. The latter signal shifted to 7.3 ppm for a *C*/50 rate and even to 12.7 ppm for an unwashed electrode. The above-mentioned experimental results clearly represent the influence of a variety of electrochemical and structural parameters on the $^7$Li chemical shifts. The changes in the structural properties might also be reflected in the ionic conductivities in the electrolyte systems. In the present work, we have conducted $^{6/7}$Li magic-angle spinning (MAS) NMR measurements and $^7$Li SLR experiments to elucidate the structural details and dynamic properties of lithiated MCMBs with and without surface modification.

## Results and Discussion

Figure 1 shows scanning electron microscopy (SEM) images of a) pristine MCMB and b) MCMB decorated with 4.7 wt % copper particles (MCMB_Cu). The copper particles are visible as bright spots on the graphitic surface. They are distributed homogeneously on the carbon surface, spherical in shape, and their average size is between 50 and 300 nm.

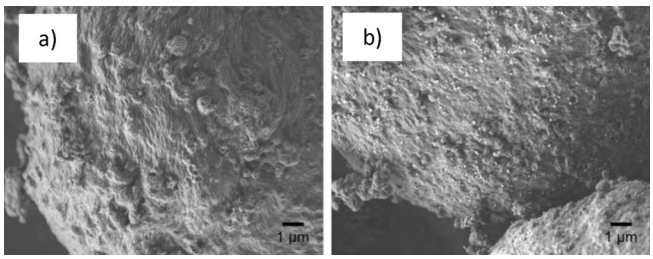


***Figure 1.*** SEM images of a) MCMB and b) MCMB_Cu at a magnification ratio of 7500.

In Figure 2 locally resolved energy-dispersive X-ray spectroscopy (EDX) of copper depositions on graphite and the corresponding SEM image at a magnification ratio of 10000 are displayed. Absorbed oxygen was detected as a homogeneous distribution over the entire sample surface and could not be assigned to the areas of the copper decorations specifically. Therefore, it is proven that the depositions consist of elemental copper.

All investigations of modified MCMB shown in this work were performed using MCMB with a copper content of 4.7 wt %. Licht et al. investigated the influence of the copper content on the electrochemical behavior of MCMB and found an optimum at this value.[5] Cyclic voltammetry measurements were performed to identify different electrochemical reactions. Figure 3 shows cyclic voltammograms (CV) of the first cycle of both pristine (black) and modified (grey) MCMB at a scan rate of 0.2 mV $s^{-1}$ between 0.02 and 1.5 V vs. $Li/Li^+$. The corresponding peak pairs with a formal potential of approximately 0.2 V for both materials are characteristic of the intercalation of lithium into the graphite lattice. The current density of the corresponding peak pair of

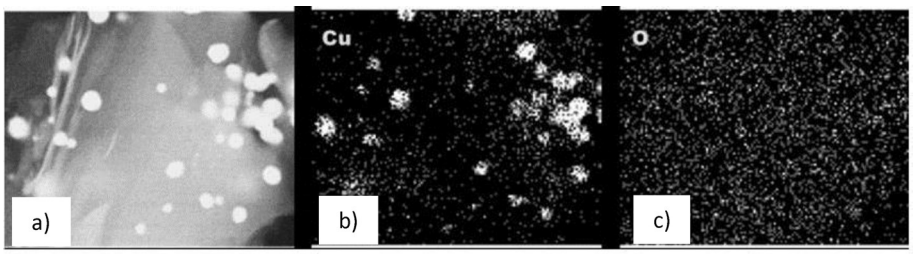


***Figure 2.*** a) SEM image of MCMB at a magnification ratio of 10000_Cu, b) locally resolved EDX of copper, and c) locally resolved EDX of oxygen.

  

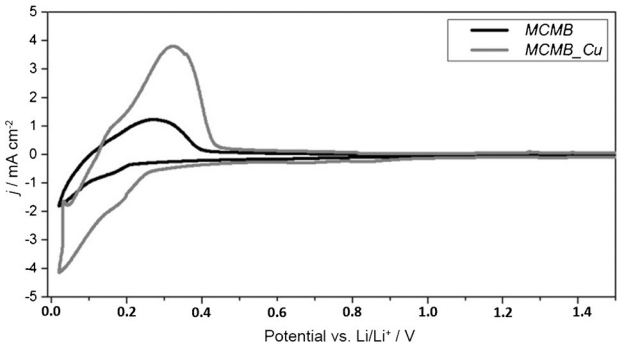


***Figure 3.*** Cyclic voltammograms of MCMB and MCMB_Cu at a scan rate of 0.02 $mV s^{-1}$ between 0.02 and 2.0 V vs. $Li/Li^+$

MCMB_Cu is two times higher, which indicates more-efficient intercalation behavior and a therefore higher capacity. The corresponding irreversible cathodic peak at approximately 0.6 V, which is reported to be characteristic for solvent co-intercalation[1,5] does not appear in the CV of MCMB. This corresponds well to the fact that the thickness of MCMB particles is increased compared to flake graphite.

The long-term cyclability was tested for both MCMB and MCMB_Cu over 150 cycles and is displayed in Figure 4. MCMB shows a lower capacity from the very beginning as well as a significant decrease during cycling. MCMB_Cu shows approximately 30 mAh $g^{-1}$ higher capacity and is stable over the tested cycles. As reported by Winter et al., thicker particles such as MCMB suppress the co-intercalation.[7] Due to the form of the thick MCMB particles, solvent co-intercalation has no major effect on the MCMB. Therefore, other effects than the suppression of cointercalation due to better SEI formation must make important contributions to the improved electrochemical behavior. It could also be possible, that the copper depositions increase the electric conductivity of the material. Concerning the high electrical conductivity of graphite, this effect is assumed to be relatively small, though it may play a major role in materials with low electric conductivity, for example, lithium titanate ($Li_4Ti_5O_{12}$).[21]

Li NMR spectroscopy can distinguish between different Li species incorporated in the carbon matrix. $^7Li$ NMR spectra (Figure 5a,b) and $^6Li$ MMR spectra (Figure 5c,d) are shown

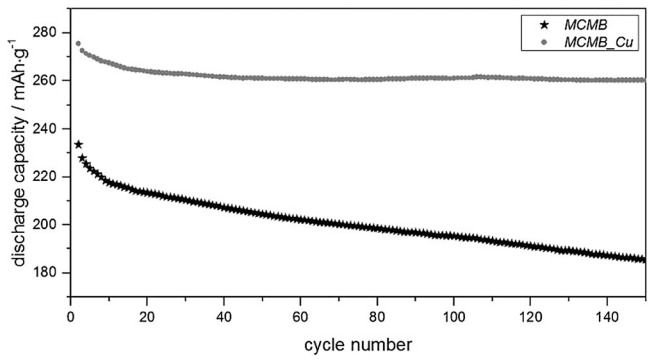


***Figure 4.*** Cycling profile of MCMB and MCMB_Cu over 150 cycles, with a rate of C/2 between 2 and 0.02 V vs. $Li/Li^+$

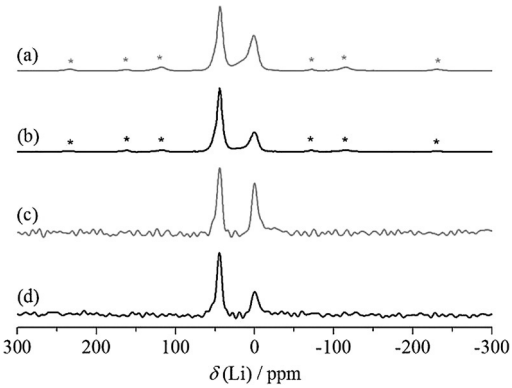


***Figure 5.*** $^7Li$ (27 kHz; a and b) and $^6Li$ (20 kHz; c and d) MAS NMR spectra of Li-intercalated MCMB samples collected at 14 T at $^7Li$ and $^6Li$ Larmor frequencies of 233.3 and 88.34 MHz, respectively. The spectra in a) and c) are from MCMB_Cu and b) and d) are from MCMB

both for MCMB and MCMB_Cu. The Li NMR spectra show mainly two peaks centered at 45 and 0 ppm. The signal at 45 ppm is characteristic for $LiC_6$. The peak centered at 0 ppm belongs to ionic lithium species typically observed in the SEI. For example $LiPF_6$, LiF, and different lithium carbonates constitute the SEI mainly. The relative intensity of the SEI signal in MCMB_Cu is increased compared to that in MCMB, which supports the assumption that the character of the SEI is changed due to the copper modification. It is assumed that the copper particles catalyze the SEI formation. There was no signal observed corresponding to lithium-copper alloy, and NMR is very sensitive to even small amounts of metallic lithium;[22] therefore an interaction of copper and lithium is unlikely. Additionally, the electrochemical reaction of copper with lithium does not take place in the measured potential range. To identify the fluorine-containing decomposition products of the SEI formation, we have conducted $^{19}F$ MAS NMR experiments on both MCMB and MCMB_Cu. Figure 6 shows the two MAS spectra which depict identical fluorine positions for $LiPF_6$ (−72 ppm), polyvinylidene fluoride (PVDF, −92 ppm, −115 ppm), HF (−152 ppm) and LiF (−207 ppm).[23,24] The broad signal at −186 ppm corresponds to poly(carbon monofluoride)[25] and it is more intense for MCMB than for MCMB_Cu. The broad signals between −100 and −200 ppm may also have less intense contributions belonging to C–F moieties, which could be formed during the SEI formation. The possible breakdown products with C–F connectivities are described by Leifer et al.[26] The intensity of the signal at 152 ppm decreases for MCMB_Cu compared to MCMB, and the reduced amount of HF might reflect a lower moisture content due to copper decompositions, as suggested by Wu et al.[27] However, the signals of PVDF do not seem to be affected by the surface modification.

To investigate the change in the hydrogen coordination in PVDF after cycling we conducted $^1H$ MAS NMR experiments on pristine PVDF, cycled MCMB, and MCMB_Cu. Pristine PVDF shows two characteristic signals centered at 5.5 and 1.1 ppm as shown by the dotted line in Figure 7c,

  

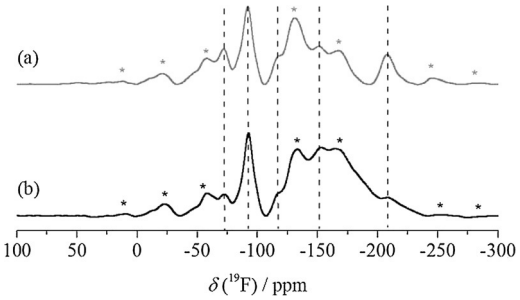


***Figure 6.*** $^{19}$F MAS (at 20 kHz) NMR spectra of Li-intercalated a) MCMB_Cu and b) MCMB. The spectra were collected at 14 T at a $^{19}$F Larmor frequency of 564.86 MHz. The dashed lines indicate the isotropic peaks and the asterisks represent the spinning side-bands.

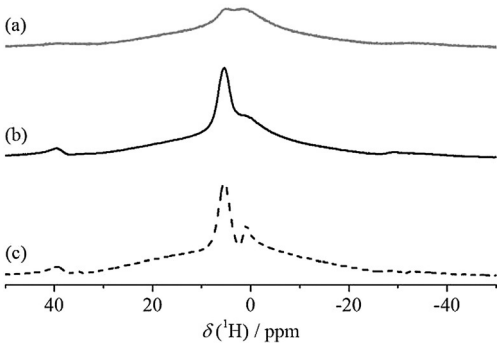


***Figure 7.*** $^{1}$H MAS (at 20 kHz) NMR spectra of Li intercalated a) MCMB_Cu, b) MCMB, and c) PVDF. The spectra were collected at 14 T at a $^{19}$F Larmor frequency of 564.86 MHz.

they correspond to –CHF (5.9 ppm) and –$CH_2$ (1.5 ppm).[28] The line shape of the MCMB sample does not deviate significantly from pristine PVDF, although a rounding of the edges was observed, probably due to a slightly different distribution of dipolar interactions. However, the $^{1}$H NMR spectrum of MCMB_Cu is strongly affected by the SEI formation. This also implies increased SEI formation due to the catalytic nature of the copper particles.

Spin-lattice relaxation experiments are used to elucidate the ion dynamics in lithium-ion conductors. These experiments can provide information on ionic jump rates, activation barriers, and dimensionalities. The activation energies for Li diffusion are obtained from the Arrhenius-type behavior of diffusion-induced relaxation rates (see, e.g., Ref. [8]). The ion dynamics in $LiC_6$ prepared using chemical synthesis have been studied by Langer et al.[16] using relaxometry. SLR experiments in the rotating frame yielded an activation energy of 0.57 eV for lithium diffusion in $LiC_6$. We compared the relaxation behaviors of lithium for $LiC_6$ in MCMB_Cu and MCMB (electrochemically prepared). We estimated an activation energy of 0.52 eV which agrees with the results from Langer et al,[15] and we did not observe any significant change in lithium dynamics in $LiC_6$ between MCMB and MCMB_Cu. However, the lithium motion in the SEI showed a change in activation energy. Figure 8 shows the $^{7}$Li $T_1$ relaxation rates of both samples as a function of temperature.

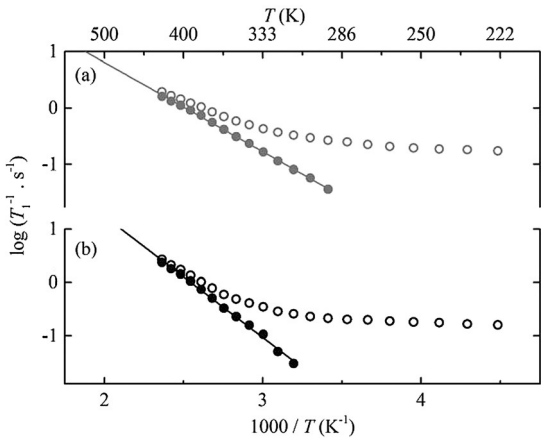


***Figure 8.*** Temperature dependent $^{7}$Li SLR rates (in the laboratory frame) of the SEI signal of a) MCMB_Cu and b) MCMB. The open symbols show the experimental data points with an influence from the non-diffusive background contribution to the relaxation. The solid symbols represent purely diffusion-induced relaxation after the subtraction of the background. The solid lines show the Arrhenius fit yielding activation energies of 0.31 (for MCMB_Cu) and 0.45 eV (for MCMB). The experiments were conducted at a $^{7}$Li Larmor frequency of 233.3 MHz.

In the case of MCMB_Cu the activation energy was 0.31 eV whereas that for MCMB was 0.45 eV. This indicates easier lithium diffusion in the SEI in the case of MCMB_Cu compared to MCMB. Although the internal diffusion between the graphitic layers ($LiC_6$) is not affected by the surface modification, the SEI seems to be influenced by it. $^{19}$F measurements showed a different composition of the SEI of MCMB_Cu as compared to MCMB, which could be responsible for the improved diffusion of lithium ions in the SEI. It is also possible, that a change in structure of the SEI occurs due to the surface modification, which can also affect the mobility of lithium ions.

## Conclusions

Electrochemical cyclability tests of MCMB and MCMB_Cu revealed an improved capacity and long cycle life for MCMB_Cu. As demonstrated in cyclic voltammetry, the thick MCMB particles suppress solvent co-intercalation. Therefore, other reasons for the improved characteristics are relevant. NMR measurements reveal different reasons for the improved behavior. Lithium NMR shows an increased intensity of the peak at 0 ppm, corresponding to SEI formation for MCMB_Cu, showing an increased formation of SEI for the modified material. This is in good agreement with $^{13}$C NMR spectra, which reveal an increased decomposition of PVDF for MCMB_Cu. Therefore, it seems likely that the copper deposition catalyzes the SEI formation. $^{19}$F measurements show that the composition of the SEI is changed as well. Particularly interesting is that the amount of HF is significantly reduced for MCMB_Cu, which supports the assumption that the copper particles reduce moisture in the material, which can cause decomposition of the active materials and gas formation. $^{7}$Li spin-lattice relaxation measure-

  

ments yield a lower activation energy for lithium ion diffusion in the SEI of MCMB_Cu as compared to MCMB, pointing at improved transport of lithium ions through the interface. All described effects of the copper modification have a positive influence on cycling behavior.

In summary, the effects identified in this work, accountable for the electrochemical improvement of MCMB_Cu compared to MCMB, are an increased SEI formation, a facilitated diffusion of lithium ions through the SEI, and reduced moisture. Other effects, not proven in this work, for example, the increased electric conductivity, may be of importance as well.

## Experimental Section

### Synthesis

The modification of MCMB with copper depositions was prepared as reported by Licht et al. 2015.[5] MCMB was mixed with copper formate [$Cu(HCOO)_2{\cdot}4H_2O$, Alfa Aesar, 98%] using a Retsch mixer mill MM 200, at a low frequency of 20 Hz for 1 h. The powder blend then was transferred into a reaction tube, heated for 30 min to 100 °C, and then heated for 1 h at 300 °C under argon flow. MCMB with 4.7 wt% copper was synthesized.

### Electrode preparation

Electrode tapes were prepared from a composition of 95% MCMB (active material) and 5% sodium carboxy methycellulose (Na-CMC, binder) and were used as electrodes for cycle stability measurements and cyclic voltammetry. To produce adequate amounts of samples for NMR measurements, electrode pellets were produced. Active material (90%) and binder polyvinylidene fluoride (PVDF, 10%) were pressed into pellets ($p \approx 1.3$ kbar), with a copper net as current collector. All electrodes were dried in a Büchi oven under an oil-pump vacuum ($p < 10^{-1}$ mbar) at 130 °C for 24 h. All cells with NMR samples were dissembled under argon atmosphere. The electrodes were washed with diethylene carbonate (DEC) and *N*-methyl-2-pyrrolidone (NMP) to remove the conductive salt and binder.

### Electrochemical measurements

The electrochemical measurements were performed in Swagelok cells. For cyclic voltammetry, T-cells with a three-electrode setup and a glass fiber separator (Machery-Nagel MN QF-10) were used. The cycling measurements were conducted in a two-electrode setup with polypropylene fleece (Freudenberg FS2190) as a separator. In all setups lithium foils (Sigma–Aldrich, 99.9%) were used as counter and reference electrodes. The separators were immersed in a 3:7 ethylene carbonate (EC)/diethylene carbonate (DEC) mixture with 1 M $LiPF_6$ as conductive salt (BASF LP47). Cycling tests were performed at a rate of *C*/2 with a preceding formation step at *C*/20 for 2 cycles. NMR samples were intercalated at a rate of *C*/60. To avoid aging effects, samples were cycled for only one cycle.

### NMR

All solid-state NMR experiments were performed at a static magnetic field 14 T using a Bruker Avance III 600 spectrometer. The Larmor frequencies for $^1$H, $^6$Li, $^7$Li, and $^{19}$F nuclei in this field were 600.31, 88.34, 233.30, and 564.86 MHz, respectively. The high-resolution experiments were conducted using 2.5 mm double resonance MAS probes. The samples were spun at spinning frequencies of 20–30 kHz using zirconia rotors. For $^7$Li MAS experiments, 15 s of recycle delays were used for 64 transients. Long recycle delays of 200 s were employed for $^6$Li MAS experiments. The $^7$Li spin-lattice relaxation experiments were performed using the standard saturation recovery pulse sequence under static conditions in the temperature range between 273 and 403 K. The samples for the static NMR experiments were packed in vacuum-sealed quartz tubes. $^1$H and $^{19}$F experiments were performed using 10 s of recycle delay and 8 and 320 transients, respectively. All MAS experiments were conducted under inert dry nitrogen conditions. The chemical standardization and pulse calibration were performed for $^{6/7}$Li and $^1$H using dilute LiCl solution and adamantane, respectively. Polycrystalline $CaF_2$ was used as a $^{19}$F secondary standard.

## Acknowledgements

*We thank the Niedersächsisches Ministerium für Wissenschaft und Kultur (MWK) for the financial support of this work within Graduiertenkolleg Energiespeicher und Elektromobilität Niedersachsen (GEENI, ZN2783). We thank Kai Volgmann for technical support with the NMR measurements. We gratefully acknowledge the supply of MCMB by MTI Corporation.*

**Keywords:** electrochemistry · graphite · lithium-ion batteries · nuclear magnetic resonance · cyclic voltammetry

[1] K. Guo, Q. Pan, L. Wang, S. Fang, *J. Appl. Electrochem.* **2002**, *32*, 679–685.
[2] H. Huang, E. Kelder, J. Schoonman, *J. Power Sources* **2001**, *97-8*, 114–117.
[3] H. Wang, M. Yoshio, *J. Power Sources* **2001**, *93*, 123–129.
[4] C.-C. Yang, J.-Y. Shih, M.-Y. Wu, *Energy Procedia* **2014**, *61*, 1428–1433.
[5] B. K. Licht, F. Homeyer, K. Bösebeck, M. Binnewies, P. Heitjans, *Z. Phys. Chem.* **2015**, *229*, 1415–1427.
[6] R. Alcántara, F. J. Fernández Madrigal, P. Lavela, J. L. Tirado, J. M. Jiménez Mateos, C. Gómez de Salazar, R. Stoyanova, E. Zhecheva, *Carbon* **2000**, *38*, 1031–1041.
[7] M. Winter, P. Novák, A. Monnier, *J. Electrochem. Soc.* **1998**, *145*, 428–436.
[8] C. V. Chandran, P. Heitjans, *Ann. Rep. NMR Spectrosc.* **2016**, *89*, 1–102.
[9] K. Zaghib, K. Tatsumi, Y. Sawada, S. Higuchi, H. Abe, T. Ohsaki, *J. Electrochem. Soc.* **1999**, *146*, 2784–2793.
[10] Y. Wang, V. Yufit, X. Guo, E. Peled, S. Greenbaum, *J. Power Sources* **2001**, *94*, 230–237.
[11] M. Letellier, F. Chevallier, M. Morcrette, *Carbon* **2007**, *45*, 1025–1034.
[12] J. Conard, H. Estrade, *Mater. Sci. Eng.* **1977**, *31*, 173–176.
[13] P. Freiländer, P. Heitjans, H. Ackermann, B. Bader, G, Kiese, A. Schirmer, H.-J. Stöckmann, C. van der Marel, A. Magerl, H. Zabel, *Z. Phys. Chem.* **1987**, *151*, 93–101.
[14] A. Schirmer, P. Heitjans, *Z. Naturforsch.* **1995**, *50a*, 643–652.
[15] M. Schmid, C. Goze-Bac, S. Krämer, S. Roth, M. Mehring, C. Mathis, P. Petit, *Phys. Rev. B* **2006**, *74*, 073416.
[16] J. Langer, V. Epp, P. Heitjans, F. A. Mautner, M. Wilkening, *Phys. Rev. B* **2013**, *88*, 094304.

  

[17] S. Thinius, M. M. Islam, P. Heitjans, T. Bredow, *J. Phys. Chem. C* **2014**, *118*, 2273–2280.
[18] K. Tatsumi, T. Akai, T. Imamura, K. Zaghib, N. Iwashita, S. Higuchi, Y. Sawada, *J. Electrochem. Soc.* **1996**, *143*, 1923–1930.
[19] S. Gautier, E. Frackowiak, J. Machnikowski, J. Conrad, J. N. Rouzaud, F. Beguin, *Am. Carbon. Soc. Carbon Conf. Archiv.* **1997**, 148–149. See: http://acs.omnibooksonline.com (accessed August 2016).
[20] R. Alcántara, G. F. Oritz, P. Lavela, J. L. Tirado, R. Stoyanova, E. Zecheva, *Chem. Mater.* **2006**, *18*, 2293–2301.
[21] W. Iwaniak, J. Fritzsche, M. Zukalová, R. Winter, M. Wilkening, P. Heitjans, *Def. Diff. Forum.* **2009**, *282–292,* 565–570.
[22] C. Tsai, V. Roddatis, C. V. Chandran, Q. Ma, S. Uhlenbruck, M. Bram, P. Heitjans, O. Guillon, *ACS Appl. Mater. Interfaces* **2016**, *8*, 10617–10626.
[23] A. V. Plakhotnyk, L. Ernst, R. Schmutzler, *J. Fluorine Chem.* **2005**, *126*, 27–31.
[24] N. Dupré, M. Cuisinier, D. Guyomard, *Electrochem. Soc. Interface* **2011**, *20*, 61–67.
[25] T. R. Krawietz, J. F. Haw, *Chem. Commun.* **1998**, 2151–2152.
[26] N. Leifer, M. C. Smart, G. K. S. Prakash, L. Gonzalez, L. Sanchez, K. A. Smith, P. Bhalla, C. P. Grey, S. G. Greenbaum, *Electrochem. Soc.* **2011**, *158*, A471–A480.
[27] Y. Wu, C. Jiang, C. Wan, E. Tsuchida, *Electrochem. Commun.* **2000**, *2*, 626–629.
[28] S. Ando, R. K. Harris, P. Holstein, S. A. Reinsberg, K. Yamauchi, *Polymer* **2001**, *42*, 8137– 8151.

Received: March 23, 2016
Revised: May 31, 2016
Published online on September 4, 2016

  